Superfluid Signatures in a Dissipative Quantum Point Contact

Huang, Meng-Zi; Mohan, Jeffrey; Visuri, Anne-Maria; Fabritius, Philipp; Talebi, Mohsen; Wili, Simon; Uchino, Shun; Giamarchi, Thierry; Esslinger, Tilman

How to cite

HUANG, Meng-Zi et al. Superfluid Signatures in a Dissipative Quantum Point Contact. In: Physical review letters, 2023, vol. 130, n° 20, p. 200404. doi: 10.1103/PhysRevLett.130.200404

This publication URL: https://archive-ouverte.unige.ch/unige:174335

Publication DOI: 10.1103/PhysRevLett.130.200404

Superfluid Signatures in a Dissipative Quantum Point Contact

Meng-Zi Huang,[1,*,†] Jeffrey Mohan,[1,†] Anne-Maria Visuri,[2] Philipp Fabritius,[1] Mohsen Talebi,[1] Simon Wili,[1] Shun Uchino,[3] Thierry Giamarchi,[4] and Tilman Esslinger[1]

[1]*Institute for Quantum Electronics, ETH Zürich, 8093 Zürich, Switzerland*
[2]*Physikalisches Institut, University of Bonn, Nussallee 12, 53115 Bonn, Germany*
[3]*Advanced Science Research Center, Japan Atomic Energy Agency, Tokai 319-1195, Japan*
[4]*Department of Quantum Matter Physics, University of Geneva, 24 quai Ernest-Ansermet, 1211 Geneva, Switzerland*

(Received 6 October 2022; revised 13 February 2023; accepted 13 April 2023; published 19 May 2023; corrected 25 August 2023)

We measure superfluid transport of strongly interacting fermionic lithium atoms through a quantum point contact with local, spin-dependent particle loss. We observe that the characteristic non-Ohmic superfluid transport enabled by high-order multiple Andreev reflections transitions into an excess Ohmic current as the dissipation strength exceeds the superfluid gap. We develop a model with mean-field reservoirs connected via tunneling to a dissipative site. Our calculations in the Keldysh formalism reproduce the observed nonequilibrium particle current, yet do not fully explain the observed loss rate or spin current.

DOI: 10.1103/PhysRevLett.130.200404

The interplay between coherent Hamiltonian dynamics and incoherent, dissipative dynamics emerging from coupling to the environment leads to rich phenomena in open quantum systems [1–3], including the quantum Zeno effect [4–9], emergent dynamics [10–15], and dissipative phase transitions [16–21]. Moreover, an important question is how many-body coherence competes with dissipation by dephasing or particle loss. Directed transport between two reservoirs offers an advantageous setup for studying this competition since dissipation can be applied locally without perturbing the many-body states in the reservoirs [22]. So far, studies on dissipation in solid-state systems have focused on dephasing [23–25]. More recently, quantum gases have become versatile platforms to study interacting many-body physics and to engineer novel forms of dissipation [2,4], though previous transport experiments on dissipation have focused on weakly interacting systems [26–28].

Engineered dissipation in strongly correlated fermionic systems, while only starting to be explored theoretically [20,29], opens interesting themes such as its competition with superfluidity where pairing and many-body coherence are key. While the Josephson effect is an archetype of superfluid transport, irreversible currents between superfluids are highly nontrivial but less studied in cold-atom systems. A prime example is the excess current between two superconductors [30] or superfluids [31] through a high-transmission quantum point contact (QPC) under a chemical potential bias where the Josephson current is suppressed. Because of the superfluid gap Δ, direct quasiparticle transport is suppressed when the chemical potential difference $\Delta\mu$ between the reservoirs is smaller than 2Δ [illustrated in Fig. 1(d)]. Instead, this energy barrier can be overcome by cotunneling of many Cooper pairs $n_{\mathrm{pair}} \geq \Delta/\Delta\mu$, each providing an energy $2\Delta\mu$ [32,33]. This process is known as multiple Andreev reflections (MAR) [34–37]. The robustness of MAR to dissipation is

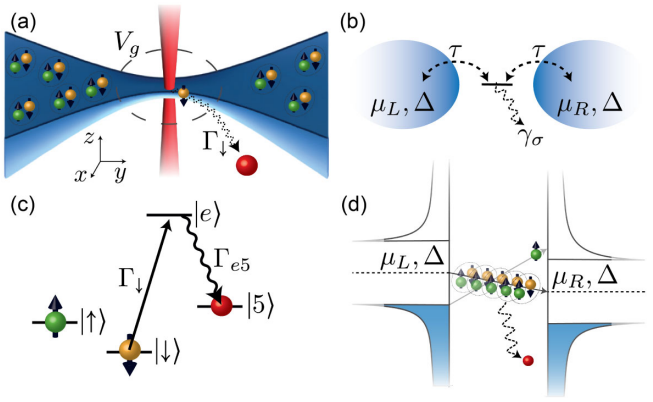

FIG. 1. (a) Two-terminal transport setup of a strongly interacting Fermi gas with a dissipation beam resonant with $|\downarrow\rangle$ at the center of a 1D channel. A gate beam (dashed circle) exerts an attractive potential V_g that determines the superfluid gap Δ and the number of transport modes n_m. (b) Theoretical model where the channel is modeled by a single, lossy site tunnel coupled to BCS reservoirs. (c) Dissipation scheme showing the relevant atomic energy levels. $|\downarrow\rangle$ is optically excited by the dissipation beam to $|e\rangle$, which decays predominantly to an auxiliary ground state $|5\rangle$ that quickly leaves the system. (d) Illustration of MAR in a superconducting QPC: transporting a quasiparticle requires energy to overcome the gap 2Δ, which is enabled by cotunneling of many pairs, each providing a small energy $2(\mu_L - \mu_R)$. The quasiparticle and constituents of the pairs experience dissipation, inhibiting this process.

an interesting open question, especially for pair-breaking particle loss acting on only one spin state, since the very existence of MAR relies on many-body coherence between the spins.

In this Letter, we address this question by experimentally and theoretically studying the influence of spin-dependent particle loss on superfluid transport. We use a strongly correlated Fermi gas—a superfluid with many-body pairing—in a transport setup with two reservoirs connected by a QPC and apply controllable local particle loss at the contact. We find that, surprisingly, the superfluid behavior survives for dissipation strengths larger than Δ—the energy scale responsible for the observed current. This result is reproduced by a minimal model that includes both superconductivity and dissipation written in the Keldysh formalism.

Experiment.—We prepare a degenerate Fermi gas of ^{6}Li in a harmonic trap in a balanced mixture of the first- and third-lowest hyperfine ground states, labeled $|\downarrow\rangle$ and $|\uparrow\rangle$. The atomic cloud has typical total atom numbers $N = N_\downarrow + N_\uparrow = 195(14) \times 10^3$, temperatures $T = 100(2)$ nK, and Fermi temperatures $T_F = h\bar{\nu}_{\mathrm{trap}}(3N)^{1/3}/k_B = 391(10)$ nK, where h is the Planck constant, k_B the Boltzmann constant, and $\bar{\nu}_{\mathrm{trap}} = 98(2)$ Hz the geometrical mean of the harmonic trap frequencies. Using a pair of repulsive, TEM_{01}-like beams intersecting at the center of the cloud, we optically define two half-harmonic reservoirs connected by a quasi-1D channel with transverse confinement frequencies $\nu_x = 10(2)$ kHz and $\nu_z = 9.9(2)$ kHz, realizing a QPC illustrated in Fig. 1(a). We apply a magnetic field of 689.7 G to address the spins' Feshbach resonance, giving rise to a fermionic superfluid in the densest parts of the cloud at the contacts to the 1D channel. An attractive Gaussian beam propagating along z acts as a "gate" potential V_g, which increases the local chemical potential at the contacts. It enhances the local degeneracy $T/T_F \sim 0.03$ [38] well into the superfluid phase and determines both the superfluid gap Δ and the number n_m of occupied transverse transport modes in the contact. Both Δ and n_m can be computed from the known potential energy landscape and equation of state [38] and are approximately $\Delta \approx k_B \times 1.4\ \mu\mathrm{K} \approx \hbar \times 184\ \mathrm{ms}^{-1}$ and $n_m \approx 3$ in this Letter.

We engineer spin-dependent particle loss with a tightly focused beam at the center of the 1D channel [Fig. 1(a)] that optically pumps $|\downarrow\rangle$ to an auxiliary ground state $|5\rangle$ [Fig. 1(c)], which interacts weakly with the two spin states and is lost due to photon recoil [38]. This leads to a controllable particle dissipation rate of $|\downarrow\rangle$ atoms given by the peak photon scattering rate $\Gamma_\downarrow$ with no observable heating in the reservoirs. While this loss beam is far off-resonant for $|\uparrow\rangle$, causing no dissipation in the absence of interatomic interactions, we observe loss of $|\uparrow\rangle$ in the strongly interacting regime studied here [38]. Even at the strongest dissipation, the system lifetime is over a second,

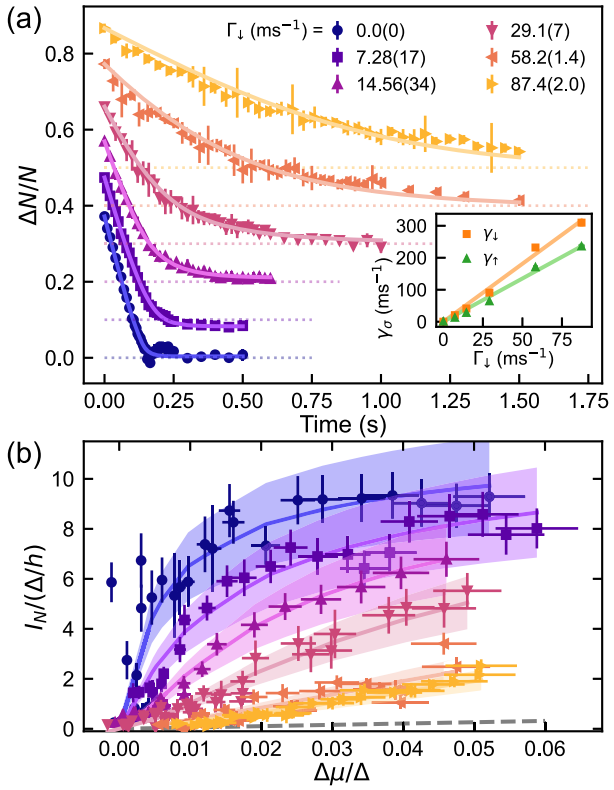

FIG. 2. (a) Time evolution of particle imbalance for various dissipation strengths $\Gamma_\downarrow$. Solid curves are fits of the theoretical model and the datasets are vertically offset by 0.1 for clarity. Error bars represent 1σ statistical uncertainty of 4 to 5 repetitions. The fitted dissipation γ_σ ($\gamma_\uparrow \equiv 0.72\gamma_\downarrow$) for each curve is plotted versus $\Gamma_\downarrow$ in the inset, showing a linear relation (solid lines are linear fits). (b) Numerically extracted current-bias relation for the same datasets in units of the gap $\Delta \approx \hbar \times 184\ \mathrm{ms}^{-1}$. The dashed line indicates the maximum normal conductance $2n_m/h$. Error bars include uncertainties in the conversion to reduced units. The uncertainties in the calculated current, represented by the shaded bands, originate mostly from the number of transmission modes n_m.

much longer than the timescale of a detectable transport of 10^3 atoms via MAR $\sim 10^3\ h/\Delta \sim 30$ ms.

We induce particle transport from the left to the right reservoir by preparing an atom number imbalance $\Delta N = N_L - N_R$ that generates a chemical potential bias $\Delta\mu = \Delta\mu(\Delta N, N, T)$ given by the system's equation of state [38]. $\Delta\mu$ drives a current $I_N = -\dot{\Delta N}/2$ from left to right that causes ΔN to decay over time t. The dynamics of $\Delta N(t)/N(t)$ for various $\Gamma_\downarrow$ are plotted in Fig. 2(a). From each trace, we numerically extract the current-bias relation $I_N(\Delta\mu)$, shown in Fig. 2(b) in units of the superfluid gap Δ [38].

For weakly interacting spins, the decay of $\Delta N(t)$ at arbitrary $\Gamma_\downarrow$ is exponential since a QPC coupling two Fermi liquids has a linear (Ohmic) current-bias relation $I_N = G\Delta\mu$. The conductance G is quantized in units of $2/h$

(2 comes from spin) but can be renormalized to a smaller value by dissipation [27,58]. In contrast, we observe that the decay of ΔN at $\Gamma_\downarrow = 0$ deviates strongly from an exponential and the corresponding current-bias relation $I_N(\Delta\mu)$ is highly nonlinear, consistent with previous observations in the strongly interacting regime [31]. In fact, this nonlinearity is a signature of superfluidity. Specifically, for ballistic superconducting QPCs [36], the current is approximately $I_N \approx G\Delta\mu + I_N^{\mathrm{exc}}$ where the normal current $G\Delta\mu \approx 2n_m\Delta\mu/h$ is carried by quasiparticles. The excess current $I_N^{\mathrm{exc}} \approx (16/3)n_m\Delta/h$ carried by the Cooper pairs is given by the superfluid gap Δ—the natural energy scale in this system. The dominance of the excess current over the normal current can be seen in $\Delta N(t)/N$ with $\Gamma_\downarrow = 0$: It decays almost linearly in time, indicating that the current is nearly independent of $\Delta\mu$. We do not expect Josephson oscillations (as in Ref. [50,52]) here since the irreversible current (MAR) damps the reversible Josephson current below our experimental resolution [51,54].

We now turn to the question of the influence of dissipation on the superfluid transport. At low $\Gamma_\downarrow$, superfluidity is still evident from the linear initial decay of ΔN, which gives way to exponential behavior at low bias where the MAR responsible for transport become higher order. The effect of dissipation is clearer in the extracted current-bias relations shown in Fig. 2(b). As dissipation strength increases, the initial current (largest $\Delta\mu$) reduces as does the concavity of the curve. The current-bias relation eventually approaches a straight line at high dissipation, yet the slope is still significantly larger than the normal conductance $2n_m/h$ [dashed line in Fig. 2(b)]. We argue below, after fitting our theoretical model to the data, that this excess conductance, albeit linear, is a signature of the MAR process. An increased temperature leading to a suppressed gap can result in similar anomalous conductance [31,73,76–78], though we can exclude this effect here from the absence of temperature increase in the reservoirs. Another possible contribution to the linear conductance in a unitary Fermi gas arises from pair tunneling coupled to collective modes in the superfluid [51,56]. However, it is expected to be on the order of $2/h$ per mode, thus negligible compared to the MAR contribution even at strong dissipation. This is also consistent with the small linear conductance (slope at large bias $\sim 2n_m/h$) in the observed current-bias relation at $\Gamma_\downarrow = 0$.

Theoretical model and fit.—We have developed a mean-field model based on previous work [31] by adding an atom loss process within the Lindblad master equation framework [38]. The two reservoirs are treated as BCS superfluids, and transport through the channel is modeled by single-particle tunneling with amplitude τ from either reservoir onto a dissipative site between them [Fig. 1(b)]. The dissipation is modeled with a Lindblad operator $\hat{L}_\sigma = \sqrt{\gamma_\sigma}\hat{d}_\sigma$ proportional to the site's fermionic annihilation operator $\hat{d}_\sigma$ with a rate γ_σ for each spin $\sigma = \downarrow, \uparrow$, i.e., as a pure particle loss process that is uncorrelated between the two spins. $\gamma_\downarrow$ is directly related to $\Gamma_\downarrow$ as our results below show, while $\gamma_\uparrow$ is included phenomenologically to match the experimental observation that $|\uparrow\rangle$ is also lost due to the strong interaction.

To compute nonequilibrium observables such as I_N, we use the Keldysh formalism extended to dissipative systems [20,41–45,79]. The time integral of the theoretical current $I_N^K(\Delta\mu, \tau, \gamma_\downarrow, \gamma_\uparrow)$ along with the equation of state $\Delta\mu(\Delta N, N, T)$ yields the model's prediction for the time evolution of the particle imbalance $\Delta N^K(t, \tau, \gamma_\downarrow, \gamma_\uparrow)$. Here, $N(t)$ is obtained from an exponential fit to the data [38]. For simplicity, we model a single transport mode and obtain the net current by multiplying by the number of modes $\Delta\dot{N}^K = -2n_m I_N^K$. Although the formalism can treat nonzero temperatures, we simplify the calculation by using zero temperature since $k_B T/\Delta < 0.08$.

Because of the spin-dependent loss, a spin imbalance builds up, leading to a magnetization imbalance $\Delta M = \Delta N_\downarrow - \Delta N_\uparrow \neq 0$ that can drive additional particle current. Nevertheless, ΔM remains small ($\Delta M/N < 0.07$) for all our data and its effect on I_N is negligible [38]. Moreover, the model predicts a spin current 1 order of magnitude below the observed value, and therefore does not fully describe the spin-dependent transport. In this Letter, we focus on spin-averaged particle transport.

We perform a least-squares fit of $\Delta N^K(t, \tau, \gamma_\downarrow, \gamma_\uparrow)$ to the measured $\Delta N(t)$ to extract the model parameters τ, $\gamma_\downarrow$, and $\gamma_\uparrow$. In our case of low bias and ballistic channel, I_N^K is sensitive only to the sum $\gamma = \gamma_\uparrow + \gamma_\downarrow$. Therefore, to avoid overfitting, we fix the ratio $\gamma_\uparrow/\gamma_\downarrow = r$ to the average measured ratio of the atom loss rates of the two spin states $r = \dot{N}_\uparrow/\dot{N}_\downarrow = 0.72(4)$ [38]. As the gap Δ is the natural unit of current and bias, the estimation of Δ in the experimental system is crucial for quantitative comparison to the model. However, the spatially varying gap in the potential energy landscape of the experiment (crossover from the 3D reservoirs to the 1D channel) is not explicitly modeled. Motivated by this and an experimental uncertainty of about 6% in the potential energy of the gate beam, we fit a multiplicative correction factor η_g on the gate potential V_g, which strongly affects both our estimate of Δ in the most degenerate point in the system and n_m [38]. Since the system is identical in each dataset except for the dissipation strength, we first fit the $\Gamma_\downarrow = 0$ data with $\gamma_\downarrow = \gamma_\uparrow = 0$ to find τ and η_g, which determine the concavity of $I_N^K(\Delta\mu)$ and the timescale of $\Delta N^K(t)$, respectively. We then fit the single parameter $\gamma_\downarrow$ with fixed r, τ, and η_g for subsequent sets. The systematic error in η_g is the dominant source of uncertainty in our theoretical calculations.

The fits for each dataset are plotted as solid lines in Figs. 2(a) and 2(b). With this fitting procedure, we find

$\eta_g = 0.98(6)$, $\Delta/k_B = 1.4(1)$ μK, and $n_m = 2.6(5)$. The fitted τ determines the energy linewidth of the dissipative site $\Gamma_d \propto \tau^2$ [38], which in units of the gap is $\Gamma_d = 5.9(4)\Delta$. Independent measurements with different values of ν_x and V_g produce similar results for η_g and Γ_d within 20%. The large value of Γ_d reflects the near-perfect transmission of the ballistic channel as the limit $\Gamma_d \to \infty$ is equivalent to perfect transparency $\alpha \to 1$ in a QPC model with direct tunneling between the reservoirs [31,38,40]. In principle, the energy ϵ_d of the dissipative site is another free parameter. Because of the large linewidth, however, the model is insensitive to changes of ϵ_d within the physically meaningful range $|\epsilon_d| < \Delta$. There are thus no resonant effects as in a weakly coupled quantum dot, and we fix $\epsilon_d = 0$. For the same reason, we do not consider any on-site interaction.

The fitted $\gamma_\downarrow$ and $\gamma_\uparrow$ versus $\Gamma_\downarrow$, plotted in the inset of Fig. 2(a), show that the effective dissipation strength is approximately proportional to the photon scattering rate as expected. The fitted slope $\gamma_\downarrow = 3.6\Gamma_\downarrow$ is of order 1, corroborating the use of our single-site model where only one $|\downarrow\rangle$ fermion fits into the dissipation beam at a time. In accordance, the dissipation beam's waist $w_y = 1.31(2)$ μm is comparable to the Fermi wavelength in the channel $\lambda_F \approx 2$ μm.

Robustness of superfluid transport to dissipation.—Supported by the overall fit to the data, our calculations provide insight into the observed flattening of the nonlinear current-bias relation: a plausible scenario is that dissipation suppresses higher-order MAR processes while allowing lower-order MAR ($n_{\text{pair}} < \Delta/\Delta\mu$) to contribute [38]. Despite the nonlinearity disappearing as dissipation increases, the current still originates from MAR. A benchmark for this superfluid signature is the excess current above the possible normal current $2n_m\Delta\mu/h$. To see this quantitatively, we replot the measured and calculated current in Fig. 3(a) versus $\Gamma_\downarrow$ at a few bias values including the initial bias $\Delta\mu/\Delta \approx 0.05$ ($n_{\text{pair}} \approx 20$) down to $\Delta\mu/\Delta \approx 0.005$ ($n_{\text{pair}} \approx 200$). The fitted model is shown in solid curves using the fitted linear relationship between $\gamma_\downarrow$ and $\Gamma_\downarrow$ in the inset of Fig. 2(a). The observed current well exceeds the upper bound of normal current (dashed lines in corresponding colors) for all biases, indicating the persistence of the MAR-enabled current. Moreover, the excess current decays smoothly with dissipation and gives no indication of a dissipative phase transition but rather shows a dissipative superfluid-to-normal crossover (cf. Ref. [6,25]).

Since the current $I_N = -(\dot{N}_L - \dot{N}_R)/2$ could in principle arise purely from an asymmetric particle loss, we verify that the conserved current I^{cons}—the atoms transported through the QPC without being lost—exceeds the upper bound for the normal current at dissipation strengths above the gap. This is shown in Fig. 3(b) where we plot the data for the largest bias together with bounds for I^{cons}. These bounds are obtained by writing $\dot{N}_{L/R} = \mp I^{\text{cons}} - I^{\text{loss}}_{L/R}$, where $I^{\text{loss}}_{L/R}$ is the dissipation-induced current into the vacuum [45], and thus $I_N = I^{\text{cons}} + (I^{\text{loss}}_L - I^{\text{loss}}_R)/2$. Assuming the worst-case scenario—maximally asymmetric loss—leads to $I^{\text{cons}} \in [I_N - \dot{N}/2, I_N + \dot{N}/2]$. The excess conserved current shows that the system preserves its superfluid signature up to $\hbar\gamma \gtrsim \Delta$.

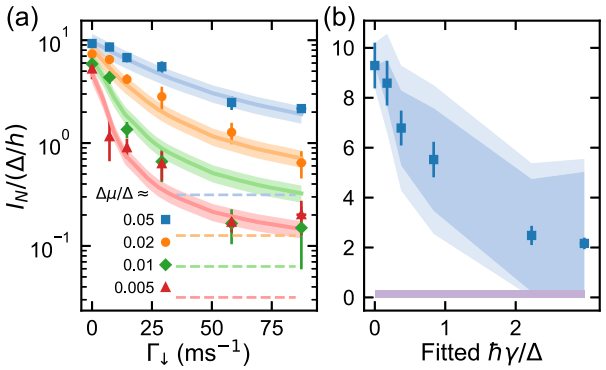

FIG. 3. (a) Measured current vs dissipation strength at different biases. The theoretical calculations are shown as solid curves with uncertainties in lighter colors. Dashed lines represent upper bounds of normal-state currents $2n_m\Delta\mu/h$. (b) Same data at $\Delta\mu/\Delta \approx 0.05$ with bounds on the conserved current $I^{\text{cons}} \in [I_N - \dot{N}/2, I_N + \dot{N}/2]$ indicated by the shaded area (lighter color represents the uncertainty). The horizontal axis is the fitted $\gamma = \gamma_\downarrow + \gamma_\uparrow$ in units of the gap to illustrate the effective strength of the dissipation. The conserved current is above the normal current (bounds represented by the horizontal bar), showing superfluid character even for the strongest dissipation.

Atom loss rate.—Finally, we compare the theoretical model to the experiment in terms of the total atom loss rate $\dot{N} = \dot{N}_L + \dot{N}_R$. In the Keldysh formalism, computing steady-state observables involves an integration over energy. Because our model assumes reservoirs with linear dispersion, we introduce a high energy cutoff Λ. The current only has contributions from energies constrained by $\Delta\mu$ and Δ, and is therefore independent of the cutoff when $\Lambda > \Delta, \Delta\mu$. The atom loss rate on the other hand depends on the cutoff and converges to its maximum value when $\Lambda \gg \Gamma_d$. We find that a single Λ cannot reproduce the observed atom loss rate at different dissipation [shown in Fig. 4(a) for $\Delta\mu/\Delta \approx 0.05$]: The atom loss rate saturates as dissipation increases, while the calculated loss rate increases almost linearly with dissipation in the measured range. In particular, $\Lambda \gtrsim 20\Delta$ is needed to reproduce the data at weak dissipation, close to the converged value, while $\Lambda \approx 5\Delta$ reproduces the data at strong dissipation. This discrepancy is shown in Fig. 4(b), which plots the Λ needed to reproduce $\dot{N}$ at each measured $\Gamma_\downarrow$. Physically, this means that additional mechanisms not included in the model suppress the occupation of the dissipative site and hence the loss rate. The calculations do predict a saturation

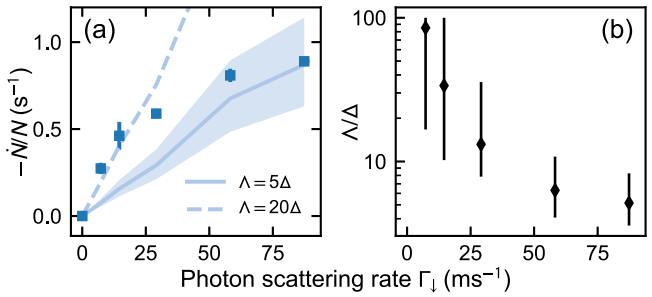

FIG. 4. (a) Normalized atom loss rate vs dissipation strength at the initial bias, which shows saturation at high dissipation. The curves are calculations with different energy cutoff Λ. Uncertainties due to Δ and n_m are represented by the shaded area (only shown for the solid curve). (b) The energy cutoff needed to reproduce each data point with nonzero dissipation, indicating the underlying energy dependence neglected in our model. The error bars account for uncertainties in Δ, n_m, and γ.

of $\dot{N}$ at an order of magnitude higher dissipation strength followed by a slow decrease of $\dot{N}$ versus $\Gamma_\downarrow$—a signature of the quantum Zeno effect [4–6]. We do not observe this nonmonotonicity, and expect it to be washed out due to the lack of energy resolution in $\dot{N}$ [80] and the finite width of the dissipative beam.

Conclusion.—We have shown a remarkable robustness of the MAR processes responsible for the current through a QPC between two superfluids of strongly interacting Fermi gas under spin-dependent particle loss. We observed no critical behavior, which contrasts with other types of superfluid-suppressing perturbations such as moving defects [81–83], magnetic fields in superconductors [84], and photon absorption by superconducting nanowire single-photon detectors [85]. While our most significant observations are captured by our model, deviations from the theory point to the importance of strong interactions in the unitary regime and energy dependence of the channel and dissipation. These effects can be probed in future studies on thermoelectricity [57,86], spin conductance [76,87], and correlated loss [88–91] in similar systems.

We thank Alexander Frank for technical support and Lukas Rammelmüller for providing us with his calculations of the finite-temperature equation of state of the spin-polarized unitary Fermi gas. We also thank Giulia Del Pace, Eugene Demler, Alex Gómez Salvador, Martón Kanász-Nagy, and Alfredo Levy Yeyati for discussions. M.-Z. H., J. M., P. F., M. T., S. W., and T. E. acknowledge the Swiss National Science Foundation (Grants No. 182650, No. 212168, and No. NCCR-QSIT) and European Research Council advanced grant TransQ (Grant No. 742579) for funding. A.-M. V. acknowledges funding from the Deutsche Forschungsgemeinschaft (DFG, German Research Foundation) in particular under Project No. 277625399—TRR 185 (B3) and Project No. 277146847—CRC 1238 (C05) and Germany's Excellence Strategy—Cluster of Excellence Matter and Light for Quantum Computing (ML4Q) EXC2004/1—390534769. S. U. acknowledges MEXT Leading Initiative for Excellent Young Researchers, JSPS KAKENHI (Grant No. JP21K03436), and Matsuo Foundation. T. G. acknowledges support from the Swiss National Science Foundation (Grant No. 2000020-188687).

*mhuang@phys.ethz.ch
†M.-Z. H. and J. M. contributed equally to this work.

[1] H.-P. Breuer, F. Petruccione *et al.*, *The Theory of Open Quantum Systems* (Oxford University Press, New York, 2002).
[2] A. J. Daley, Quantum trajectories and open many-body quantum systems, Adv. Phys. **63**, 77 (2014).
[3] Y. Ashida, Z. Gong, and M. Ueda, Non-Hermitian physics, Adv. Phys. **69**, 249 (2020).
[4] G. Barontini, R. Labouvie, F. Stubenrauch, A. Vogler, V. Guarrera, and H. Ott, Controlling the Dynamics of an Open Many-Body Quantum System with Localized Dissipation, Phys. Rev. Lett. **110**, 035302 (2013).
[5] B. Zhu, B. Gadway, M. Foss-Feig, J. Schachenmayer, M. L. Wall, K. R. A. Hazzard, B. Yan, S. A. Moses, J. P. Covey, D. S. Jin, J. Ye, M. Holland, and A. M. Rey, Suppressing the Loss of Ultracold Molecules Via the Continuous Quantum Zeno Effect, Phys. Rev. Lett. **112**, 070404 (2014).
[6] T. Tomita, S. Nakajima, I. Danshita, Y. Takasu, and Y. Takahashi, Observation of the Mott insulator to superfluid crossover of a driven-dissipative Bose-Hubbard system, Sci. Adv. **3**, e1701513 (2017).
[7] H. Fröml, A. Chiocchetta, C. Kollath, and S. Diehl, Fluctuation-Induced Quantum Zeno Effect, Phys. Rev. Lett. **122**, 040402 (2019).
[8] P. E. Dolgirev, J. Marino, D. Sels, and E. Demler, Non-Gaussian correlations imprinted by local dephasing in fermionic wires, Phys. Rev. B **102**, 100301(R) (2020).
[9] M. Will, J. Marino, H. Ott, and M. Fleischhauer, Controlling superfluid flows using dissipative impurities, SciPost Phys. **14**, 064 (2023).
[10] M.-A. Miri and A. Alù, Exceptional points in optics and photonics, Science **363**, eaar7709 (2019).
[11] F. Letscher, O. Thomas, T. Niederprüm, M. Fleischhauer, and H. Ott, Bistability Versus Metastability in Driven Dissipative Rydberg Gases, Phys. Rev. X **7**, 021020 (2017).
[12] N. Dogra, M. Landini, K. Kroeger, L. Hruby, T. Donner, and T. Esslinger, Dissipation-induced structural instability and chiral dynamics in a quantum gas, Science **366**, 1496 (2019).
[13] R. Bouganne, M. Bosch Aguilera, A. Ghermaoui, J. Beugnon, and F. Gerbier, Anomalous decay of coherence in a dissipative many-body system, Nat. Phys. **16**, 21 (2020).
[14] D. Dreon, A. Baumgärtner, X. Li, S. Hertlein, T. Esslinger, and T. Donner, Self-oscillating pump in a topological dissipative atom–cavity system, Nature (London) **608**, 494 (2022).
[15] L.-N. Wu, J. Nettersheim, J. Feß, A. Schnell, S. Burgardt, S. Hiebel, D. Adam, A. Eckardt, and A. Widera, Dynamical

phase transition in an open quantum system, arXiv:2208.05164.
[16] E. M. Kessler, G. Giedke, A. Imamoglu, S. F. Yelin, M. D. Lukin, and J. I. Cirac, Dissipative phase transition in a central spin system, Phys. Rev. A **86**, 012116 (2012).
[17] T. Fink, A. Schade, S. Höfling, C. Schneider, and A. Imamoglu, Signatures of a dissipative phase transition in photon correlation measurements, Nat. Phys. **14**, 365 (2018).
[18] S. Helmrich, A. Arias, G. Lochead, T. M. Wintermantel, M. Buchhold, S. Diehl, and S. Whitlock, Signatures of self-organized criticality in an ultracold atomic gas, Nature (London) **577**, 481 (2020).
[19] F. Ferri, R. Rosa-Medina, F. Finger, N. Dogra, M. Soriente, O. Zilberberg, T. Donner, and T. Esslinger, Emerging Dissipative Phases in a Superradiant Quantum Gas with Tunable Decay, Phys. Rev. X **11**, 041046 (2021).
[20] K. Yamamoto, M. Nakagawa, N. Tsuji, M. Ueda, and N. Kawakami, Collective Excitations and Nonequilibrium Phase Transition in Dissipative Fermionic Superfluids, Phys. Rev. Lett. **127**, 055301 (2021).
[21] J. Benary, C. Baals, E. Bernhart, J. Jiang, M. Röhrle, and H. Ott, Experimental observation of a dissipative phase transition in a multi-mode many-body quantum system, New J. Phys. **24**, 103034 (2022).
[22] L. Amico *et al.*, Roadmap on Atomtronics: State of the art and perspective, AVS Quantum Sci. **3**, 039201 (2021).
[23] G. Schön and A. D. Zaikin, Quantum coherent effects, phase transitions, and the dissipative dynamics of ultra small tunnel junctions, Phys. Rep. **198**, 237 (1990).
[24] J. S. Penttilä, U. Parts, P. J. Hakonen, M. A. Paalanen, and E. B. Sonin, "Superconductor-Insulator Transition" in a Single Josephson Junction, Phys. Rev. Lett. **82**, 1004 (1999).
[25] A. Murani, N. Bourlet, H. le Sueur, F. Portier, C. Altimiras, D. Esteve, H. Grabert, J. Stockburger, J. Ankerhold, and P. Joyez, Absence of a Dissipative Quantum Phase Transition in Josephson Junctions, Phys. Rev. X **10**, 021003 (2020).
[26] R. Labouvie, B. Santra, S. Heun, and H. Ott, Bistability in a Driven-Dissipative Superfluid, Phys. Rev. Lett. **116**, 235302 (2016).
[27] L. Corman, P. Fabritius, S. Häusler, J. Mohan, L. H. Dogra, D. Husmann, M. Lebrat, and T. Esslinger, Quantized conductance through a dissipative atomic point contact, Phys. Rev. A **100**, 053605 (2019).
[28] W. Gou, T. Chen, D. Xie, T. Xiao, T.-S. Deng, B. Gadway, W. Yi, and B. Yan, Tunable Nonreciprocal Quantum Transport through a Dissipative Aharonov-Bohm Ring in Ultracold Atoms, Phys. Rev. Lett. **124**, 070402 (2020).
[29] F. Damanet, E. Mascarenhas, D. Pekker, and A. J. Daley, Controlling Quantum Transport via Dissipation Engineering, Phys. Rev. Lett. **123**, 180402 (2019).
[30] L. Bretheau, c. C. Girit, L. Tosi, M. Goffman, P. Joyez, H. Pothier, D. Esteve, and C. Urbina, Superconducting quantum point contacts, C. R. Phys. **13**, 89 (2012).
[31] D. Husmann, S. Uchino, S. Krinner, M. Lebrat, T. Giamarchi, T. Esslinger, and J.-P. Brantut, Connecting strongly correlated superfluids by a quantum point contact, Science **350**, 1498 (2015).
[32] R. Cron, M. F. Goffman, D. Esteve, and C. Urbina, Multiple-Charge-Quanta Shot Noise in Superconducting Atomic Contacts, Phys. Rev. Lett. **86**, 4104 (2001).
[33] J. C. Cuevas and W. Belzig, Full Counting Statistics of Multiple Andreev Reflections, Phys. Rev. Lett. **91**, 187001 (2003).
[34] G. E. Blonder, M. Tinkham, and T. M. Klapwijk, Transition from metallic to tunneling regimes in superconducting microconstrictions: Excess current, charge imbalance, and supercurrent conversion, Phys. Rev. B **25**, 4515 (1982).
[35] D. Averin and A. Bardas, AC Josephson Effect in a Single Quantum Channel, Phys. Rev. Lett. **75**, 1831 (1995).
[36] J. C. Cuevas, A. Martín-Rodero, and A. Levy Yeyati, Hamiltonian approach to the transport properties of superconducting quantum point contacts, Phys. Rev. B **54**, 7366 (1996).
[37] C. J. Bolech and T. Giamarchi, Keldysh study of point-contact tunneling between superconductors, Phys. Rev. B **71**, 024517 (2005).
[38] See Supplemental Material at http://link.aps.org/supplemental/10.1103/PhysRevLett.130.200404 for additional information on the theoretical methods, experimental procedures, and data analysis, which includes Refs. [39–75].
[39] F. Setiawan and J. Hofmann, Analytic approach to transport in superconducting junctions with arbitrary carrier density, Phys. Rev. Res. **4**, 043087 (2022).
[40] A. Martín-Rodero and A. Levy Yeyati, Josephson and Andreev transport through quantum dots, Adv. Phys. **60**, 899 (2011).
[41] A.-M. Visuri, T. Giamarchi, and C. Kollath, Symmetry-Protected Transport Through a Lattice with a Local Particle Loss, Phys. Rev. Lett. **129**, 056802 (2022).
[42] A. Kamenev, *Field Theory of Non-Equilibrium Systems* (Cambridge University Press, Cambridge, England, 2011).
[43] L. M. Sieberer, M. Buchhold, and S. Diehl, Keldysh field theory for driven open quantum systems, Rep. Prog. Phys. **79**, 096001 (2016).
[44] T. Jin, M. Filippone, and T. Giamarchi, Generic transport formula for a system driven by Markovian reservoirs, Phys. Rev. B **102**, 205131 (2020).
[45] S. Uchino, Comparative study for two-terminal transport through a lossy one-dimensional quantum wire, Phys. Rev. A **106**, 053320 (2022).
[46] B. Lu, P. Burset, and Y. Tanaka, Spin-polarized multiple Andreev reflections in spin-split superconductors, Phys. Rev. B **101**, 020502(R) (2020).
[47] A. Martín-Rodero, A. Levy Yeyati, and J. Cuevas, Microscopic theory of the phase-dependent linear conductance in highly transmissive superconducting quantum point contacts, Physica (Amsterdam) **218B**, 126 (1996).
[48] M. Tinkham, *Introduction to Superconductivity*, 2nd ed., International Series in Pure and Applied Physics (McGraw Hill, New York, 1996).
[49] K. K. Likharev, Superconducting weak links, Rev. Mod. Phys. **51**, 101 (1979).
[50] G. Del Pace, W. J. Kwon, M. Zaccanti, G. Roati, and F. Scazza, Tunneling Transport of Unitary Fermions across the Superfluid Transition, Phys. Rev. Lett. **126**, 055301 (2021).

[51] F. Meier and W. Zwerger, Josephson tunneling between weakly interacting Bose-Einstein condensates, Phys. Rev. A **64**, 033610 (2001).
[52] G. Valtolina, A. Burchianti, A. Amico, E. Neri, K. Xhani, J. A. Seman, A. Trombettoni, A. Smerzi, M. Zaccanti, M. Inguscio, and G. Roati, Josephson effect in fermionic superfluids across the BEC-BCS crossover, Science **350**, 1505 (2015).
[53] S. Krinner, D. Stadler, D. Husmann, J.-P. Brantut, and T. Esslinger, Observation of quantized conductance in neutral matter, Nature (London) **517**, 64 (2014).
[54] J. Yao, B. Liu, M. Sun, and H. Zhai, Controlled transport between Fermi superfluids through a quantum point contact, Phys. Rev. A **98**, 041601(R) (2018).
[55] S. Uchino and J.-P. Brantut, Bosonic superfluid transport in a quantum point contact, Phys. Rev. Res. **2**, 023284 (2020).
[56] S. Uchino, Role of Nambu-Goldstone modes in the fermionic-superfluid point contact, Phys. Rev. Res. **2**, 023340 (2020).
[57] D. Husmann, M. Lebrat, S. Häusler, J.-P. Brantut, L. Corman, and T. Esslinger, Breakdown of the Wiedemann-Franz law in a unitary Fermi gas, Proc. Natl. Acad. Sci. U.S.A. **115**, 201803336 (2018).
[58] M. Lebrat, S. Häusler, P. Fabritius, D. Husmann, L. Corman, and T. Esslinger, Quantized Conductance through a Spin-Selective Atomic Point Contact, Phys. Rev. Lett. **123**, 193605 (2019).
[59] M. Houbiers, H. T. C. Stoof, W. I. McAlexander, and R. G. Hulet, Elastic and inelastic collisions of ^{6}Li atoms in magnetic and optical traps, Phys. Rev. A **57**, R1497 (1998).
[60] W. Zwerger, ed., *The BCS-BEC Crossover and the Unitary Fermi Gas*, Lecture Notes in Physics No. 836 (Springer, Heidelberg, 2012).
[61] J. E. Thomas, J. Kinast, and A. Turlapov, Virial Theorem and Universality in a Unitary Fermi Gas, Phys. Rev. Lett. **95**, 120402 (2005).
[62] Y.-i. Shin, C. H. Schunck, A. Schirotzek, and W. Ketterle, Phase diagram of a two-component Fermi gas with resonant interactions, Nature (London) **451**, 689 (2008).
[63] B. A. Olsen, M. C. Revelle, J. A. Fry, D. E. Sheehy, and R. G. Hulet, Phase diagram of a strongly interacting spin-imbalanced fermi gas, Phys. Rev. A **92**, 063616 (2015).
[64] L. Rammelmüller, A. C. Loheac, J. E. Drut, and J. Braun, Finite-Temperature Equation of State of Polarized Fermions at Unitarity, Phys. Rev. Lett. **121**, 173001 (2018).
[65] M. J. H. Ku, A. T. Sommer, L. W. Cheuk, and M. W. Zwierlein, Revealing the superfluid lambda transition in the universal thermodynamics of a unitary fermi gas, Science **335**, 563 (2012).
[66] Y.-H. Hou, L. P. Pitaevskii, and S. Stringari, First and second sound in a highly elongated fermi gas at unitarity, Phys. Rev. A **88**, 043630 (2013).
[67] G. Zürn, T. Lompe, A. N. Wenz, S. Jochim, P. S. Julienne, and J. M. Hutson, Precise Characterization of ^{6}Li Feshbach Resonances Using Trap-Sideband-Resolved rf Spectroscopy of Weakly Bound Molecules, Phys. Rev. Lett. **110**, 135301 (2013).
[68] Y. Long, F. Xiong, and C. V. Parker, Spin Susceptibility Above the Superfluid Onset in Ultracold Fermi Gases, Phys. Rev. Lett. **126**, 153402 (2021).
[69] L. Rammelmüller, Y. Hou, J. E. Drut, and J. Braun, Pairing and the spin susceptibility of the polarized unitary fermi gas in the normal phase, Phys. Rev. A **103**, 043330 (2021).
[70] I. Boettcher, J. Braun, T. K. Herbst, J. M. Pawlowski, D. Roscher, and C. Wetterich, Phase structure of spin-imbalanced unitary fermi gases, Phys. Rev. A **91**, 013610 (2015).
[71] E. Scheer, N. Agraït, J. C. Cuevas, A. Levy Yeyati, B. Ludoph, A. Martín-Rodero, G. R. Bollinger, J. M. van Ruitenbeek, and C. Urbina, The signature of chemical valence in the electrical conduction through a single-atom contact, Nature (London) **394**, 154 (1998).
[72] T. Ihn, *Semiconductor Nanostructures: Quantum States and Electronic Transport* (Oxford University Press, Oxford; New York, 2010).
[73] M. Kanász-Nagy, L. Glazman, T. Esslinger, and E. A. Demler, Anomalous Conductances in an Ultracold Quantum Wire, Phys. Rev. Lett. **117**, 255302 (2016).
[74] E. Scheer, P. Joyez, D. Esteve, C. Urbina, and M. H. Devoret, Conduction Channel Transmissions of Atomic-Size Aluminum Contacts, Phys. Rev. Lett. **78**, 3535 (1997).
[75] A. Schirotzek, Y.-i. Shin, C. H. Schunck, and W. Ketterle, Determination of the Superfluid Gap in Atomic Fermi Gases by Quasiparticle Spectroscopy, Phys. Rev. Lett. **101**, 140403 (2008).
[76] S. Krinner, M. Lebrat, D. Husmann, C. Grenier, J.-P. Brantut, and T. Esslinger, Mapping out spin and particle conductances in a quantum point contact, Proc. Natl. Acad. Sci. U.S.A. **113**, 8144 (2016).
[77] S. Uchino and M. Ueda, Anomalous Transport in the Superfluid Fluctuation Regime, Phys. Rev. Lett. **118**, 105303 (2017).
[78] B. Liu, H. Zhai, and S. Zhang, Anomalous conductance of a strongly interacting Fermi gas through a quantum point contact, Phys. Rev. A **95**, 013623 (2017).
[79] A.-M. Visuri, T. Giamarchi, and C. Kollath, Nonlinear transport in the presence of a local dissipation, Phys. Rev. Res. **5**, 013195 (2023).
[80] H. Fröml, C. Muckel, C. Kollath, A. Chiocchetta, and S. Diehl, Ultracold quantum wires with localized losses: Many-body quantum zeno effect, Phys. Rev. B **101**, 144301 (2020).
[81] K. W. Madison, F. Chevy, W. Wohlleben, and J. Dalibard, Vortex Formation in a Stirred Bose-Einstein Condensate, Phys. Rev. Lett. **84**, 806 (2000).
[82] L. Sobirey, N. Luick, M. Bohlen, H. Biss, H. Moritz, and T. Lompe, Observation of superfluidity in a strongly correlated two-dimensional Fermi gas, Science **372**, 844 (2021).
[83] G. Del Pace, K. Xhani, A. Muzi Falconi, M. Fedrizzi, N. Grani, D. Hernandez Rajkov, M. Inguscio, F. Scazza, W. J. Kwon, and G. Roati, Imprinting Persistent Currents in Tunable Fermionic Rings, Phys. Rev. X **12**, 041037 (2022).
[84] E. Scheer, J. C. Cuevas, A. Levy Yeyati, A. Martín-Rodero, P. Joyez, M. H. Devoret, D. Esteve, and C. Urbina, Conduction channels of superconducting quantum point contacts, Physica (Amsterdam) **280B**, 425 (2000).

[85] C. M. Natarajan, M. G. Tanner, and R. H. Hadfield, Superconducting nanowire single-photon detectors: Physics and applications, Supercond. Sci. Technol. **25**, 063001 (2012).
[86] S. Häusler, P. Fabritius, J. Mohan, M. Lebrat, L. Corman, and T. Esslinger, Interaction-Assisted Reversal of Thermopower with Ultracold Atoms, Phys. Rev. X **11**, 021034 (2021).
[87] A.-M. Visuri, M. Lebrat, S. Häusler, L. Corman, and T. Giamarchi, Spin transport in a one-dimensional quantum wire, Phys. Rev. Res. **2**, 023062 (2020).
[88] G. B. Partridge, K. E. Strecker, R. I. Kamar, M. W. Jack, and R. G. Hulet, Molecular Probe of Pairing in the BEC-BCS Crossover, Phys. Rev. Lett. **95**, 020404 (2005).
[89] F. Werner, L. Tarruell, and Y. Castin, Number of closed-channel molecules in the BEC-BCS crossover, Eur. Phys. J. B **68**, 401 (2009).
[90] T. Paintner, D. K. Hoffmann, M. Jäger, W. Limmer, W. Schoch, B. Deissler, M. Pini, P. Pieri, G. Calvanese Strinati, C. Chin, and J. Hecker Denschlag, Pair fraction in a finite-temperature Fermi gas on the BEC side of the BCS-BEC crossover, Phys. Rev. A **99**, 053617 (2019).
[91] X.-P. Liu, X.-C. Yao, H.-Z. Chen, X.-Q. Wang, Y.-X. Wang, Y.-A. Chen, Q. Chen, K. Levin, and J.-W. Pan, Observation of the density dependence of the closed-channel fraction of a ^{6}Li superfluid, Natl. Sci. Rev. **9**, nwab226 (2021).

Correction: The equal-contribution statement for the first two authors was set incorrectly during the production cycle and has been restored as a byline footnote.